Dysfunctional Insulin Resistant/mTOR Activation Is Involved In The Formation of Pulmonary Hypertension In Pressure Overload-Induced Heart Failure

Xiaojing Wu (xiaojingwu1992@163.com)
Shenzhen University https://orcid.org/0000-0002-0590-7627

Bo Dong
Shenzhen University General Hospital

Tongxin Ni
Shenzhen University General Hospital

Junhao Hu
Chongqing Medical University

Qi Zhou
Chongqing Medical University

Research

Keywords: Pulmonary hypertension, Heart failure, Metabolomics, Insulin resistance, mTOR signaling

Posted Date: June 30th, 2021

DOI: https://doi.org/10.21203/rs.3.rs-642854/v1

Abstract

Background: Heart failure (HF) usually presents with abnormal changes of metabolisms. Pulmonary hypertension (PH) is a frequent complication of left heart dysfunction. However, the association of serum metabolic changes with PH formation remains unknown. This study analyzed changes of serum metabolomic during the development of PH in a left heart pressure overload model.

Methods: Male Sprague-Dawley rats were subjected to transverse aortic constriction (TAC) or sham surgery. Metabolomic analysis was performed on plasma samples of rats at 0 week, 3 weeks and 9 weeks after the surgery. Cardiac remodeling and heart function were determined by echocardiography. Right heart catheterization was performed to assay the mean pulmonary arterial pressure (mPAP). HE staining was performed to observe the remodeling of the myocardium and small pulmonary arteries.

Results: The rats developed compensated cardiac hypertrophy with normal mPAP at 3 weeks and PH due to HF (PH-HF) at 9 weeks with distinct metabolic pattern after TAC. Twenty-five metabolites changed in the 9-week group compared with the 3-week group. KEGG analysis suggested abnormal insulin resistance and mTOR activation during the development of PH-HF. Acetylcarnitines related to insulin resistance increased about 3 folds from 4.14 ug/ml at 3 W group to 12.04μg/ml at 9-week group. L-leucine related to mTOR activation increased 1.6-fold with a VIP of 4.08 at 9 W when compared with that of the 3 W group.

Conclusions: These results revealed distinct metabolic changes during the development of PH-HF. Dysfunctional insulin resistance and mTOR activation might be involved in the transition from compensated cardiac hypertrophy to PH-HF.

Introduction

Left heart failure (HF) is a common final outcome of left heart diseases (LHD), including hypertension, coronary artery diseases and cardiac valve diseases, which mainly affect left ventricular function and systemic circulation. However, approximately 60–70% of patients with HF develop pulmonary hypertension (PH), which is called PH due to HF (PH-HF) or PH due to LHD (PH-LHD) [1, 2]. PH is a frequent complication of HF but is difficult to recognize because it is characterized by common symptoms including shortness of breath and decreased tolerance of activity. Furthermore, nearly all multicentric clinical trials targeting pulmonary circulation in PH-HF have reported negative results [3, 4]. Currently, the early diagnosis and treatment of PH-HF is insufficient.

PH includes heterogeneous groups of diseases with multiple etiologies. In contrast to Group I PH, PH-LHD belongs to Group 2 and is believed to be caused by the retrograde transmission of the left atrial pressure to pulmonary circulation, with few characteristics of heritable tendency or familiar distributions [5]. Furthermore, during the development of left heart dysfunction, many cytokines, vasoactive substances and metabolites are responsible for the development of cardiac remodeling. Metabolic changes have been reported to appear prior to the structural changes of cardiac remodeling, and metabolic

dysregulation is considered a contributing factor to the development of HF [6, 7]. However, the metabolites correlated with pulmonary hemodynamic changes remain largely unknown.

Pulmonary vascular diseases have increasingly been recognized as a systemic disorder associated with substantial metabolic dysfunction [8, 9]. Moreover, metabolites are considered useful tools in the early diagnosis and treatment of diseases because they can be easily and noninvasively detected. To further elucidate the metabolic mechanisms of PH-HF, in this study, we used a left heart overloaded rat model induced by transverse aortic constriction (TAC) surgery and observed the correlations of metabolic patterns with pulmonary hemodynamic changes during the progression of left ventricular dysfunction. We found that the heart developed compensated cardiac hypertrophy with normal mean pulmonary arterial pressure (mPAP) at 3 weeks and PH-HF at 9 weeks after TAC surgery. The metabolic pattern can differentiate PH-HF from cardiac hypertrophy with normal mPAP. Abnormal insulin resistance and mammalian target of rapamycin (mTOR) activation might be involved in the formation of PH-HF. Our study provides important information regarding the metabolic changes involved in the development of PH-HF.

Material And Methods

TAC model

All animal experiments comply with the ARRIVE guidelines and were approved by the Ethics Committee of Animal Welfare at the Medical Centers of Chongqing Medical University (Chongqing, China) and Shenzhen University General Hospital (Guangdong, China).

Male Sprague-Dawley (SD) rats (6 weeks old, body weight 200g±20 g) were provided by the Experimental Animal Center of Chongqing Medical University and housed in the individually ventilated cage (IVC) facility at the Experimental Animal Center of Chongqing Medical University. Left ventricular remodeling and heart failure were induced by TAC as previously described [10]. Briefly, the animals were anesthetized by a single intraperitoneal injection of pentobarbital (60 mg/kg) and then placed on a heating pad of 37 ℃ to maintain body temperature. A small incision was made in the left third intercostal space, and artificial ventilation (Harvard Apparatus, USA) was set to allow direct access to the thorax. After identification of the transverse aorta, a 16-gauge needle (O.D. 1.6 mm) was placed between the right innominate artery and left common carotid artery. Aortic constriction was then performed by ligating the aorta with a 2-0 silk. The needle was removed rapidly after the aorta was tied tightly. The chest cavity and skin were stitched by a 6-0 polypropylene suture (Prolene, Ethicon). After approximately 10 more min of ventilation, when spontaneous breathing was restored, the rat was extubated and returned to the housing facility for maintenance.

Forty SD rats were randomly conducted the TAC or sham surgery. The sham group underwent the same surgical procedures as the TAC group but without ligation of the aortic arch. One animal in the sham group and one animal in the TAC group died of bleeding during the surgery. One animal in the sham group died of pneumothorax during the surgery. Finally, 18 animals in the sham group and 19 animals in

the TAC group survived and were used for the experiment. The TAC rats were subjected to further examinations at 0 week (0W, n=6), 3 weeks (3 W, n=6) and 9 weeks (9 W, n=7) respectively after surgery. Heart rate and blood pressure were assessed by measuring parameters such as blood flow, blood pressure and pulse at the base of the tail using a rat tail-cuff blood pressure system.

Echocardiography

Transthoracic echocardiography was performed after TAC surgery to examine the changes in cardiac function and remodeling. The rats were anesthetized by a single intraperitoneal injection of pentobarbital (60 mg/kg), and echocardiography was then performed with VeVo2100 (VisualSonics, Canada). The diastolic intraventricular septum, LV end diastolic diameter, diastolic posterior wall thickness, LV internal dimension in systole, and percent LV fractional shortening were assessed from M-mode images, as previously described [11].

Cardiac catheter

Hemodynamic measurements were performed at 0 W, 3 W and 9 W after the surgery, following a reported method [12]. Briefly, the rats were anesthetized by a single intraperitoneal injection of pentobarbital (60 mg/kg) and then placed on a controlled heating table. The left carotid artery and right jugular vein were both cannulated with two fluid-filled polyethylene catheters that were connected to pressure transducers. Along with the catheters inserted into the right ventricle and left ventricle, the specific pressure tracings were simultaneously recorded on a PowerLab physiologic recorder System (AD Instruments, Inc., Australia). Data were not accepted if the steady state was not reached.

Metabolomic sample preparation

Blood samples from the rats were collected in 5 ml vacutainer tubes containing the chelating agent ethylenediaminetetraacetic acid (EDTA), and then, the samples were centrifuged for 15 min (1500 g, 4 °C). Each aliquot (150 μl) of the plasma sample was stored at -80 °C until ultrahigh-performance liquid chromatography equipped with quadrupole time-off light mass spectrometry (UPLC-Q-TOF/MS) analysis. The plasma samples were thawed at 4 °C, and 100 μl aliquots were mixed with 400 μl of cold methanol/acetonitrile (1:1, v/v) to remove the protein. The mixture was centrifuged for 15 min (14000 g, 4 °C). The supernatant was dried in a vacuum centrifuge. For LC-MS analysis, the samples were redissolved in 100 μl of acetonitrile/water (1:1, v/v) solvent. For monitoring the stability and repeatability of instrument analysis, quality control (QC) samples were prepared by pooling 10 μl of each sample, and these samples were analyzed together with the other samples. The QC samples were inserted regularly and analyzed every 5 samples.

LC-MS/MS analysis

Analyses were performed using an UHPLC (1290 Infinity LC, Agilent Technologies) coupled to a quadrupole time-of-flight (AB Sciex TripleTOF 6600) in Shanghai Applied Protein Technology Co., Ltd. For HILIC separation, samples were analyzed using a 2.1 mm × 100 mm Acquity UPLC BEH 1.7 μm column

(Waters, Ireland). In both ESI positive and negative modes, the mobile phase contained A=25 mM ammonium acetate and 25 mM ammonium hydroxide in water and B= acetonitrile. The gradient was 85% B for 1 min and was linearly reduced to 65% in 11 min, reduced to 40% in 0.1 min and kept for 4 min, and then increased to 85% in 0.1 min, with a 5 min re-equilibration period employed.

The ESI source conditions were set as follows: Ion Source Gas1 (Gas1) was 60, Ion Source Gas2 (Gas2) was 60, curtain gas (CUR) was 30, source temperature was 600 ℃, and IonSpray Voltage Floating (ISVF) was ± 5500 V. In MS only acquisition, the instrument was set to acquire over the m/z range 60–1000 Da, and the accumulation time for TOF MS scan was set at 0.20 s/spectra. In auto MS/MS acquisition, the instrument was set to acquire over the m/z range of 25–1000 Da, and the accumulation time for the product ion scan was set at 0.05 s/spectra. The product ion scan was acquired using information-dependent acquisition (IDA) with high sensitivity mode selected. The parameters were set as follows: the collision energy (CE) was fixed at 35 V with ± 15 eV; declustering potential (DP) was 60 V (+) and −60 V (−); excluding isotopes within 4 Da, and candidate ions to monitor per cycle: 10.

The metabolites were further confirmed by targeted metabolomic analysis or enzyme-linked immunosorbent assays (ELISAs). For targeted metabolomic analysis, multiple reaction monitoring (MRM) transitions representing the metabolites were simultaneously monitored. Each MRM ion dwell time was 3 ms, and the total cycle time was 1.263 s. ELISA was performed according to the manufacturer's instructions.

Data processing

The raw MS data (wiff.scan files) were converted to MzXML files using ProteoWizard MSConvert before importing into freely available XCMS software. For peak picking, the following parameters were used: centWave m/z = 25 ppm, peakwidth = c (10, 60), and prefilter = c (10, 100). For peak grouping, bw = 5, mzwid = 0.025, minfrac = 0.5 were used. Collection of Algorithms of MEtabolite pRofile Annotation (CAMERA) was used for annotation of isotopes and adducts. In the extracted ion features, only the variables having more than 50% of the nonzero measurement values in at least one group were kept. Compound identification of metabolites was performed by comparing the accuracy m/z value (<25 ppm) and MS/MS spectra with an in-house database established with available authentic standards.

Statistical analysis

Statistical analysis was performed using SPSS software, version 20.0 (IBM Corp.). Continuous variables were summarized as mean ± SE and all categorical variables were expressed as proportions. Datasets containing 3 groups were first analyzed by one-way ANOVA, and significance between any two groups was further analyzed by post hoc test. For metabolomic analysis, after normalization to the total peak intensity, the processed data were uploaded before importing into SIMCA-P (version 14.1, Umetrics, Umea, Sweden), where they were subjected to multivariate data analysis, including Pareto-scaled principal component analysis (PCA) and orthogonal partial least-squares discriminant analysis (OPLS-DA). Sevenfold cross-validation and response permutation testing were used to evaluate the robustness of the

model. The variable importance in the projection (VIP) value of each variable in the OPLS-DA model was calculated to indicate its contribution to the classification. Metabolites with a VIP value >1 were further applied to Student's t-test at the univariate level to measure the significance of each metabolite. P values less than 0.05 were considered statistically significant.

Results

Changes in pulmonary hemodynamic and left ventricular remodeling

Rats of 0 W group present similar parameters including body weight, blood pressure, LV mass and thickness of the LV posterior wall (LVPW), interventricular septum (IVS), normal LV ejection fraction (LVEF) and normal mPAP compared to its sham group. Rats followed for 3 weeks after TAC surgery exhibited high blood pressure, normal LVEF and normal mPAP compared to the 0 W group. The LVPW and IVS tended to be elevated but were not significantly different. However, the cross-sectional area of cardiomyocytes increased in histological assessment, suggesting subclinical compensated cardiomyocyte hypertrophy. The rats developed significant increases in the thickness of LVPW and IVS, a decrease in LVEF and an increase in mPAP at 9 weeks compared to 3 weeks after TAC surgery (mPAP 30.08 ± 1.07 mmHg vs 14.15 ± 0.13 mmHg, $P < 0.01$). Histological assessment demonstrated thickened walls of the small pulmonary arteries in the rats at 9 weeks after TAC surgery. These data indicated that the rats developed pronounced PH-HF 9 weeks after TAC surgery (Table 1, Fig. 1).

Table 1
Echocardiographic and pulmonary hemodynamic changes of rats subjected to TAC surgery

	0 W (n = 6)	3 W (n = 6)	9 W (n = 7)
BW (g)	258 ± 18	274 ± 15	429 ± 13
HR (BPM)	385 ± 8	407 ± 3	391 ± 5
BP (mmHg)	132 ± 5.85	158 ± 16.37**	201 ± 19.35**
IVS;d(mm)	1.45 ± 0.11	1.71 ± 0.09	2.86 ± 0.34*
IVS;s(mm)	2.51 ± 0.16	2.86 ± 0.22	4.43 ± 0.29*
LVID;d(mm)	5.42 ± 0.38	5.94 ± 0.29	6.47 ± 0.88*
LVID;s(mm)	2.69 ± 0.52	2.85 ± 0.36	3.56 ± 0.62*
LVPW;d(mm)	1.44 ± 0.27	1.95 ± 0.22	2.64 ± 0.30*
LVPW;s(mm)	2.65 ± 0.17	3.04 ± 0.28	3.71 ± 0.54*
LVEDV(ul)	164.27 ± 25.78	198.61 ± 24.96	278.57 ± 43.09*
LVEF(%)	82.91 ± 5.79	86.67 ± 4.39	67.09 ± 2.61*
LVFS(%)	54.81 ± 8.25	61.09 ± 7.32	42.67 ± 4.48*
LV Mass(mg)	517.38 ± 35.26	652.28 ± 30.52	1224.96 ± 166.02*
mPAP(mmHg)	14.15 ± 0.13	15.81 ± 0.78	30.08 ± 1.07*
RVSP	21.70 ± 1.06	23.73 ± 0.97	42.65 ± 0.87*
Data presented as Mean ± SE for 0W,3W and 9W group.			
BW: Body weight;HR：Heart rate；BP：blood pressure; IVS;d: the diastolic thickness of intraventricular septum; IVS;s: the systolic thickness of intraventricular septum; LVID;d: left end diastolic diameter; LVID;s: left end systolic diameter; LVPW;d: left ventricular diastolic posterior wall thickness; LVPW;s: left ventricular systolic posterior wall thickness; :LVFS: percent left ventricular fractional shortening; LVEDV： left ventricular end diastolic volume; LVEF: left ventricular ejection fraction; LV Mass: left ventricular mass; mPAP: mean pulmonary artery pressure; RVSP: right ventricular systolic pressure；			
*P < 0.05 vs 0 W, **P < 0.01 vs 0W			

Metabolomic pattern analysis

Total ion current chromatograms of the metabolites were detected using a solvent system. The relative intensity and peaks under positive mode and negative mode were different. We did not observe any obvious differences between the QCs, suggesting that variation remained in the optimal range. OPLS-DA analysis, which served as a supervised method for pattern recognition, was then conducted to investigate the metabolite patterns of PH development. As shown in Fig. 2, groups positive for 0 W, 3 W and 9 W were separated in the OPLS-DA score plots with a satisfactory goodness of fit (0 W vs 3 W: R2 = 0.977, Q2 =

0.324; 3 W vs 9 W: R2 = 0.966, Q2 = 0.832). For the metabolites detected under negative mode, score plots for each comparison were also presented as separated clusters, along with the optimal goodness of fit (0 W vs 3 W: R2 = 0.993, Q2 = 0.435; 3 W vs 9 W: R2 = 0.985, Q2 = 0.775). These results indicated that a clear separation among groups at 0 W, 3 W and 9 W was observed on the OPLS-DA score plot, and the different metabolomic patterns can be used to separate the plasma samples into the normal, compensated left ventricular hypertrophy, and PH-HF groups.

Analysis of significantly different metabolites

To further reveal the metabolites associated with the formation of PH, we analyzed the differentially abundant metabolites. The significantly different metabolites were obtained based on the OPLS-DA analysis with VIP > 1 and P < 0.05 among groups at different time points and are shown by volcano plots (Fig. 3). The metabolic changes after TAC surgery were different at the different developmental stages of PH-HF. Thirteen metabolites, including amino acids, pyrimidine, choline and glycerophospholipids, were changed in the 3 W group compared to the 0 W group. The significantly different metabolites included 5-aminopentanoic acid, L-lysine, N6-acetyl-L-lysine and L-phenylalanine. There were 25 differentially abundant metabolites at 9 W compared with 3 W in the PH-HF group. The significantly different metabolites included L-carnitine, acetylcarnitine, cholic acid, bilirubin, creatinine, hippuric acid, glyceric acid,L-leucine and vanillin (Table 2). Metabolites of amino acids were altered depending on the developmental stage of PH-HF. L-lysine and L-phenylalanine was elevated at 3 weeks, but L-leucine increased at 9 weeks after TAC surgery. In addition, the organic metabolites, including cholic acid, bilirubin, hippuric acid and glyceric acid, changed significantly. Cholic acid and bilirubin increased but hippuric acid and glyceric acid decreased significantly at 9 W after TAC surgery compared to 3 W after surgery.

Table 2
Identified significant different metabolites between 3w and 9w

Name of metabolites	Category	VIP	FC	p
L-Carnitine	Quaternary ammonium salts	9.49	1.29	< 0.001
Acetylcarnitine	Fatty acid esters	14.65	3.24	< 0.001
L-Palmitoylcarnitine	Fatty acid esters	4.17	2.86	< 0.001
1,2-dioleoyl-sn-glycero-3-phosphatidylcholine	others	8.82	0.49	0.007
(3-Carboxypropyl)trimethylammonium cation	others	2.56	1.55	0.010
Dihomo-gamma-linolenoyl-EA	others	2.10	4.25	0.015
Uracil	Pyrimidines	1.13	0.40	0.015
Triethanolamine	Alkanolamines	1.64	4.14	0.019
SOPC	Glycerophosphocholines	1.06	1.51	0.028
1-Palmitoylglycerol	others	1.67	1.24	0.029
Bilirubin	Bilirubins	1.04	2.83	0.036
epsilon-Caprolactam	others	2.48	0.73	0.043
Confertifoline	others	4.88	0.59	< 0.001
2-Methylbenzoic acid	others	1.21	0.68	< 0.001
D(-)-beta-hydroxy butyric acid	others	4.26	4.20	0.001
Hippuric acid	Benzoic acids	3.80	0.35	0.001
Vanillin	Methoxyphenols	2.81	0.49	0.001
Pentobarbital	others	14.21	0.56	0.009
Glyceric acid	Carbohydrates and carbohydrate conjugates	2.00	0.41	0.011
3-Methoxy-4-Hydroxyphenylglycol Sulfate	Methoxyphenols	2.17	1.82	0.020
Cholic acid	Bile acids	5.08	3.22	0.021

SOPC: 1-Stearoyl-2-oleoyl-sn-glycerol 3-phosphocholine

Name of metabolites	Category	VIP	FC	p
1,4-Dihydroxybenzene	Benzenediols	1.69	0.34	0.023
D-Threitol	Carbohydrates	1.32	1.53	0.027
Dihydrothymine	Pyrimidines	1.93	0.59	0.047
L-Leucine	Amino acids	4.08	1.60	0.045
SOPC: 1-Stearoyl-2-oleoyl-sn-glycerol 3-phosphocholine				

KEGG analysis

KEGG enrichment analysis was performed to reveal the underlying mechanism of PH during the progression of left heart dysfunction. Lysine degradation was the most disturbed metabolic pathway contributing to cardiac hypertrophy at 3 W after TAC surgery. Disruptions of metabolic pathways, including pyrimidine metabolism, choline metabolism, retrograde endocannabinoid signaling, arginine and proline metabolism, linoleic acid metabolism, central carbon metabolism, alpha-linolenic acid and glycerophospholipid metabolism, were also notable in the 3 W group compared with the sham group. At 9 W after TAC surgery, in addition to similar changes, including choline metabolism, retrograde endocannabinoid signaling and central carbon metabolism, the disruptions of the insulin resistance and mTOR pathways were significant (Fig. 4). The metabolites related to insulin resistance and mTOR activation were acetylcarnitine and L-leucine, respectively. The plasma level of acetylcarnitine was further confirmed by ELISAs (sensitivity: 7.1 pg/ml, Abbexa) and L-leucine by target metabolic analysis. Consistently, the plasma levels of acetylcarnitine and L-leucine were significantly increased in the 9 W group compared with the 3 W group after TAC surgery (Fig. 5).

Discussion

PH originates from HF, and PH-HF accounts for approximately half of PH patients worldwide. Although the myocardium usually experiences metabolomic changes during cardiac dysfunction, the metabolites correlated with pulmonary hemodynamic progress remain largely unknown. The present study aimed to study the correlations of serum metabolites with the development of PH-HF. We found that the heart experienced compensated cardiomyocyte hypertrophy with normal mPAP at 3 weeks and developed PH-HF at 9 weeks after TAC surgery. The metabolomic pattern was significantly different among the sham control, compensated cardiomyocyte hypertrophy with normal mPAP, and PH-HF groups.

HF is the most common cause of PH. The development of PH is triggered by the direct retrograde transmission of the left atrial pressure to the pulmonary circulation in the initial stage. In clinical practice right heart catheterization is the gold standard for the diagnosis of PH. Echocardiogram, however, is more popular in routine examination of LHD patients. Because the sensitivity of echocardiogram for the detection of PH is low in its mild and early stages, some patients with PH-HF, in particular those with PH-HF in the early stage, might be ignored. PH has been regarded as a late complication of HF. In fact, more

evidence showed that PH might appear earlier in the progress of HF and the morbidity of PH-HF is high [1, 2]. TAC is a widely used method for left ventricular remodeling and heart failure [13]. To further understand the influence of left heart dysfunction on pulmonary circulation, in this study, by using a TAC model, we observed PH formation during the progression of left heart dysfunction. We found that the rats exhibited compensated cardiomyocyte hypertrophy with normal mPAP at 3 weeks after TAC surgery but a significant decrease in LVEF with apparent PH at 9 weeks, indicating that PH might simultaneously develop during the progression of left heart failure.

As a major part of the circulatory system, pulmonary circulation directly affects right ventricular function. However, its influence is on the whole body. PH has increasingly been recognized as a systemic disorder associated with substantial metabolic dysfunction [14]. Accumulating studies have demonstrated the relationship of metabolic syndrome with PAH [15, 16]. In our study, we found that the plasma metabolite pattern was different depending on the developmental stage of PH and left ventricular dysfunction. The metabolic pattern not only differentiates rats with early compensated cardiac hypertrophy from sham rats without TAC procedure but also differentiate PH-HF from cardiac hypertrophy without PH. The different metabolites between 0 W and 3 W showed changes in cardiac hypertrophy. Based on the criteria of VIP > 1 and P < 0.05, we found 13 different metabolites including amino acids, pyrimidines and fatty acids. The most distinct metabolites were 5-aminopentanoic acid, N6-acetyl-L-lysine, L-lysine and L-phenylalanine. With the development of left ventricular remodeling, the rats developed PH at 9 weeks. Compared with those in the 3 W group, the distinctly changed metabolites included L-carnitine, acetylcarnitine, cholic acid, bilirubin, creatinine, hippuric acid, glyceric acid, L-leucine, and vanillin. Taken together, our data indicated that the metabolites and metabolic patterns changed depending on the development of PH and HF.

In further KEGG analysis, we found that various pathways, including lysine degradation, pyrimidine metabolism, choline metabolism, protein digestion and absorption, arginine and proline metabolism, might be associated with early cardiac hypertrophy. One notably disturbed pathway was lysine degradation. More pathways, including insulin resistance and mTOR, were disturbed at 9 W after TAC surgery compared with 3 W after surgery. Despite the well-acknowledged correlation between insulin resistance and coronary artery disease, evidence linking pulmonary vascular diseases with insulin signaling was only recently reported. Moreover, mTOR is one of the intermediates produced during TG synthesis, and mTOR signaling is activated in response to physiological and pathological stimuli, e.g., hemodynamic changes secondary to pressure overload, and leads to a global increase in protein synthesis [14]. Studies have reported the important regulatory role of mTOR both in cardiac hypertrophy and pulmonary vascular remodeling [17–19]. In our study, KEGG enrichment analysis showed that both insulin resistance and mTOR were activated at 9 W after TAC surgery. One metabolite related to insulin resistance was acetylcarnitine, and L-leucine was associated with mTOR activation.

Abnormal free fatty acid (FFA) metabolism has been reported to be involved in both insulin resistance and mTOR activation [20, 21]. Proinflammatory cytokines impair suppression of adipose tissue lipolysis, leading to FFA release into the circulation, impaired insulin-stimulated muscle glucose uptake, and

decreased suppression of hepatic glucose production. Incomplete fatty acid β-oxidation and the subsequent increase in acylcarnitine species might be linked to insulin resistance. Acetylcarnitine is an acetic acid ester of carnitine that facilitates the movement of acetyl CoA into the mitochondria during fatty acid oxidation. Zheng et al. [22] reported that plasma acetylcarnitine increased in experimental rat models of PAH induced by monocrotaline. Brittan et al. [23] found that circulating fatty acid long-chain acylcarnitines are elevated in patients with PAH and associated with fatty acid accumulation in the myocardium caused by reduced fatty acid oxidation. Our study extended the observation of acylcarnitines to PH-LHD. We found that acetylcarnitines increased about 3 folds from 4.14 ug/ml at 3 W group to 12.04μg/ml at 9 W group. Moreover, mTOR acts as an inhibitor of insulin signaling [24]. One of the major cellular mechanisms responsible for FFA-induced insulin resistance involves activation of mTOR. Increased mTOR/p70S6K1 affects insulin signaling by the phosphorylation of insulin receptor substrate-1, thereby inhibiting PI3K and Akt activation [25]. The serine/threonine protein kinase Akt, which is also known as protein kinase B and is a downstream effector of PI3K, is a critical mediator of mTOR activity. Huang et al. [26] reported that high-fat and high-carbohydrate diet-induced insulin resistance was associated with increased mTOR and decreased PI3K and Akt protein levels. Thus, increased levels of acetylcarnitine might cause insulin resistance and subsequent mTOR activation, and mTOR activation further regulated insulin resistance via crosstalk mechanisms.

Branched-chain amino acids are another regulator of both insulin resistance and mTOR activation. Leucine is the most potent activator for insulin resistance [27–28]. Moreover, insulin and leucine have an additive effect on mTOR phosphorylation [29]. In particular, increased levels of acetylcarnitine cause insulin resistance [30], which might subsequently activate mTOR signaling [31]. It is therefore suggested that crosstalk among leucine, insulin resistance and mTOR might be critical in the development of PH-LHD. In our study, L-leucine increased 1.6-fold with a VIP of 4.08 at 9 W when compared with that of the 3 W group. L-leucine might mediate the crosstalk between insulin resistance and mTOR activation

Metabolomic analyses of multiple cardiovascular diseases have identified target metabolites that could provide insights into mechanisms of disease progression and potential targets. Our studies showed that during the progression of left heart dysfunction, changes in metabolites not only suggest changes in pulmonary hemodynamic parameters but also indicate that some of the metabolites might be involved in the development of PH-HF. There are some limitations in this study. Further studies should be conducted to confirm the correlations of serum metabolite changes with pulmonary hemodynamic progress in patients. Moreover, PH and cardiac remodeling might share similar metabolic regulatory mechanisms. The abnormal regulation of insulin resistance and mTOR activation in the formation of PH, as well as their relationships with cardiac remodeling, should be extensively studied.

Conclusions

By using a rat model of TAC our study showed that the metabolic pattern and metabolites were significantly different between compensated cardiac hypertrophy and PH-HF. As shown by the transition from compensated cardiomyocyte hypertrophy to PH-HF, the dysfunctional insulin resistance and mTOR

activation might participate in the development of PH. Our study provides a novel method for noninvasively distinguishing PH from HF by metabolic patterns and metabolite assays. The associated metabolites might be potential targets for the treatment of PH-HF.

Declarations

Ethics approval and consent to participate

All animal experiments comply with the ARRIVE guidelines and were approved by the Ethics Committee of Animal Welfare at the Medical Centers of Chongqing Medical University (Chongqing, China) and Shenzhen University General Hospital (Guangdong, China).

Consent for publication

Not applicable.

Availability of data and materials

The datasets generated and/or analyzed during the current study are not publicly available due to privacy or ethical restrictions, but are available from the corresponding author on reasonable request.

Competing interest

The authors declare that there is no conflict of interest.

Funding

This study was supported by grants from the National Scientific Foundation of China (NSFC 81270109, 91539104), the Natural Scientific Foundation of Guangdong Province (2019A1515011421), the Natural Scientific Foundation of Shenzhen (JCYJ20190808122207499) and Shenzhen Municipal Commission of Science and Technology Innovation (ZDSYS20190902093401689). The funders had no role in study design, in collection, analysis and interpretation of data, in writing of the manuscript, and in decision to submit the article for publication.

Authors' Contributions

QZ and XW contributed equally to this work and share the corresponding authorship. QZ and XW contributed to the study conception design and design. Material preparation and data collection were performed by JHH and TN. XW, BD and TN performed statistical analysis. The draft of the manuscript was written by XW. All authors read and approved the final manuscript.

Acknowledgments

The authors would like to thank members of Shanghai Applied Protein Technology for assistance on metabolomic LC-MS/MS analysis.

References

1. Ghio S, D'Alto M, Badagliacca R, et al. Pulmonary hypertension in left heart disease: The need to continue to explore. Int J Cardiol.2019,288:132–134.
2. Rosenkranz S, Lang IM, Blindt R, et al. Pulmonary hypertension associated with left heart disease: Updated Recommendations of the Cologne Consensus Conference 2018. Int J Cardiol. 2018,**272S**:53–62.
3. Kido K, Coons JC. Efficacy and Safety of the Use of Pulmonary Arterial Hypertension Pharmacotherapy in Patients with Pulmonary Hypertension Secondary to Left Heart Disease: A Systematic Review. Pharmacotherapy. 2019;39:929–45.
4. Cao JY, Wales KM, Cordina R. Pulmonary vasodilator therapies are of no benefit in pulmonary hypertension due to left heart disease: A meta-analysis. Int J Cardiol. 2018;273:213–20.
5. Breitling S, Ravindran K, Goldenberg NM. The pathophysiology of pulmonary hypertension in left heart disease. Am J Physiol Lung Cell Mol Physiol. 2015;309:L924–41.
6. Tuomainen T, Tavi P. The Role of Cardiac Energy Metabolism in Cardiac Hypertrophy and Failure. Exp Cell Res. 2017;360:12–8.
7. Sun H, Olson KC, Gao C, et al. Catabolic Defect of Branched-Chain Amino Acids Promotes Heart Failure. Circulation. 2016;133:2038–49.
8. Culley MK, Chan SY. Mitochondrial metabolism in pulmonary hypertension: beyond mountains there are mountains. J Clin Invest. 2018;128:3704–15.
9. Chan SY, Rubin LJ. Metabolic dysfunction in pulmonary hypertension: from basic science to clinical practice. Eur Respir Rev. 2017;26:170094.
10. Liu Q, Hu H, Hu T, et al. STVNa attenuates right ventricle hypertrophy and pulmonary artery remodeling in rats induced by transverse aortic constriction. Biomed Pharmacother. 2018;101:371–8.
11. Kimura A, Ishida Y, Furuta M, et al. Protective Roles of Interferon-γ in Cardiac Hypertrophy Induced by Sustained Pressure Overload. J Am Heart Assoc. 2018;7:e008145.
12. Deten A, Millar H, Zimmer HG. Catheterization of pulmonary artery in rats with an ultraminiature catheter pressure transducer. Am J Physiol Heart Circ Physiol. 2003;285:H2212–7.
13. deAlmeida AC, van Oort RJ, Wehrens XH. Transverse aortic constriction in mice. J Vis Exp. 2010;38:1729.
14. Assad TR, Hemnes AR. Metabolic Dysfunction in Pulmonary Arterial Hypertension. Curr Hypertens Rep. 2015;17:20.
15. Ussavarungsi K, Thomas CS, Burger CD. Prevalence of metabolic syndrome in patients with pulmonary hypertension. Clin Respir J. 2017;11:721–6.
16. Maron BA, Leopold JA, Hemnes AR. Metabolic syndrome, neurohumoral modulation, and pulmonary arterial hypertension. Br J Pharmacol. 2020;177:1457–71.

17. Xu L, Brink M. mTOR, cardiomyocytes and inflammation in cardiac hypertrophy. Biochim Biophys Acta. 2016;1863:1894–903.
18. Tang H, Wu K, Wang J, et al. Pathogenic Role of mTORC1 and mTORC2 in Pulmonary Hypertension. JACC Basic Transl Sci. 2018;3:744–62.
19. Liu P, Gu Y, Luo J, et al. Inhibition of Src activation reverses pulmonary vascular remodeling in experimental pulmonary arterial hypertension via Akt/mTOR/HIF-1 signaling pathway. Exp Cell Res. 2019;380:36–46.
20. Matoba A, Matsuyama N, Shibata S, et al. The free fatty acid receptor 1 promotes airway smooth muscle cell proliferation through MEK/ERK and PI3K/Akt signaling pathways. Am J Physiol Lung Cell Mol Physiol. 2018;314:L333–48.
21. Arner P, Rydén M. Fatty Acids, Obesity and Insulin Resistance. Obes Facts. 2015;8:147–55.
22. Zheng HK, Zhao JH, Yan Y, et al. Metabolic reprogramming of the urea cycle pathway in experimental pulmonary arterial hypertension rats induced by monocrotaline. Respir Res. 2018;19:94.
23. Brittain EL, Talati M, Fessel JP, et al. Fatty Acid Metabolic Defects and Right Ventricular Lipotoxicity in Human Pulmonary Arterial Hypertension. Circulation. 2016;133:1936–44.
24. Yoon MS. The Role of Mammalian Target of Rapamycin (mTOR) in Insulin Signaling. Nutrients. 2017;9:1176.
25. Yao H, Han X, Han X. The cardioprotection of the insulin-mediated PI3K/Akt/mTOR signaling pathway. Am J Cardiovasc Drugs. 2014;14:433–42.
26. Huang S, Tang N, Zhao H, et al. Effect of electrical stimulation combined with diet therapy on insulin resistance via mTOR signaling. Mol Med Rep. 2019;20:5152–62.
27. Lynch CJ, Adams SH. Branched-chain amino acids in metabolic signalling and insulin resistance. Nat Rev Endocrinol. 2014;10:723–36.
28. Satomi S, Morio A, Miyoshi H, et al. Branched-chain amino acids-induced cardiac protection against ischemia/reperfusion injury. Life Sci. 2020;245:117368.
29. Yang J, Dolinger M, Ritaccio G, et al. Leucine stimulates insulin secretion via down-regulation of surface expression of adrenergic α2A receptor through the mTOR (mammalian target of rapamycin) pathway: implication in new-onset diabetes in renal transplantation. J Biol Chem. 2012;287:24795–806.
30. Miyamoto Y, Miyazaki T, Honda A, et al. Retention of acetylcarnitine in chronic kidney disease causes insulin resistance in skeletal muscle. J Clin Biochem Nutr. 2016;59:199–206.
31. Walker AJ, Price JB, Borreggine K, et al. Insulin-stimulated mTOR activation in peripheral blood mononuclear cells associated with early treatment response to lithium augmentation in rodent model of antidepressant-resistance. Transl Psychiatry. 2019;9:113.

Figures

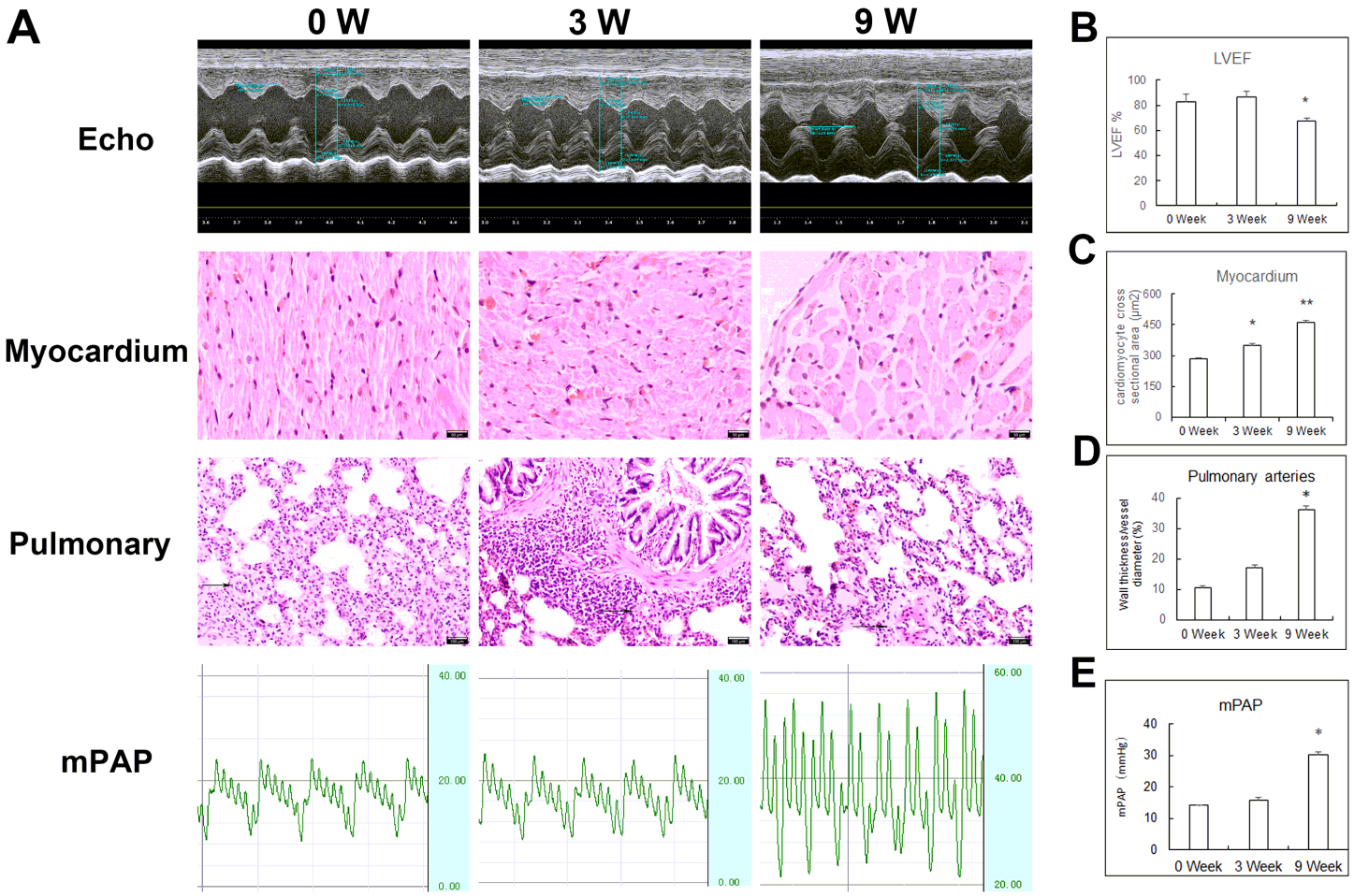

Figure 1

Remodeling of left ventricular myocardium and small pulmonary arteries at 0, 3 and 9 weeks after TAC surgery. A: Representative images of echocardiograms，Hematoxylin/eosin （HE） staining of myocardium and small pulmonary arteries，and mean pulmonary artery pressure（mPAP）assayed by right cardiac catheter. Bar was 100μm for HE staining of myocardium，Bar was 50μm for HE staining of pulmonary tissue. B，Left ventricular ejection fraction （LVEF）；C，Cross sectional area of cardiomyocyte；D，Wall thickness / vessel diameter of small pulmonary arteries；E，Changes of mPAP. n=6 for 0W and 3 W groups; n=7 for 9 W group. * p＜0.05, ** p＜0.01

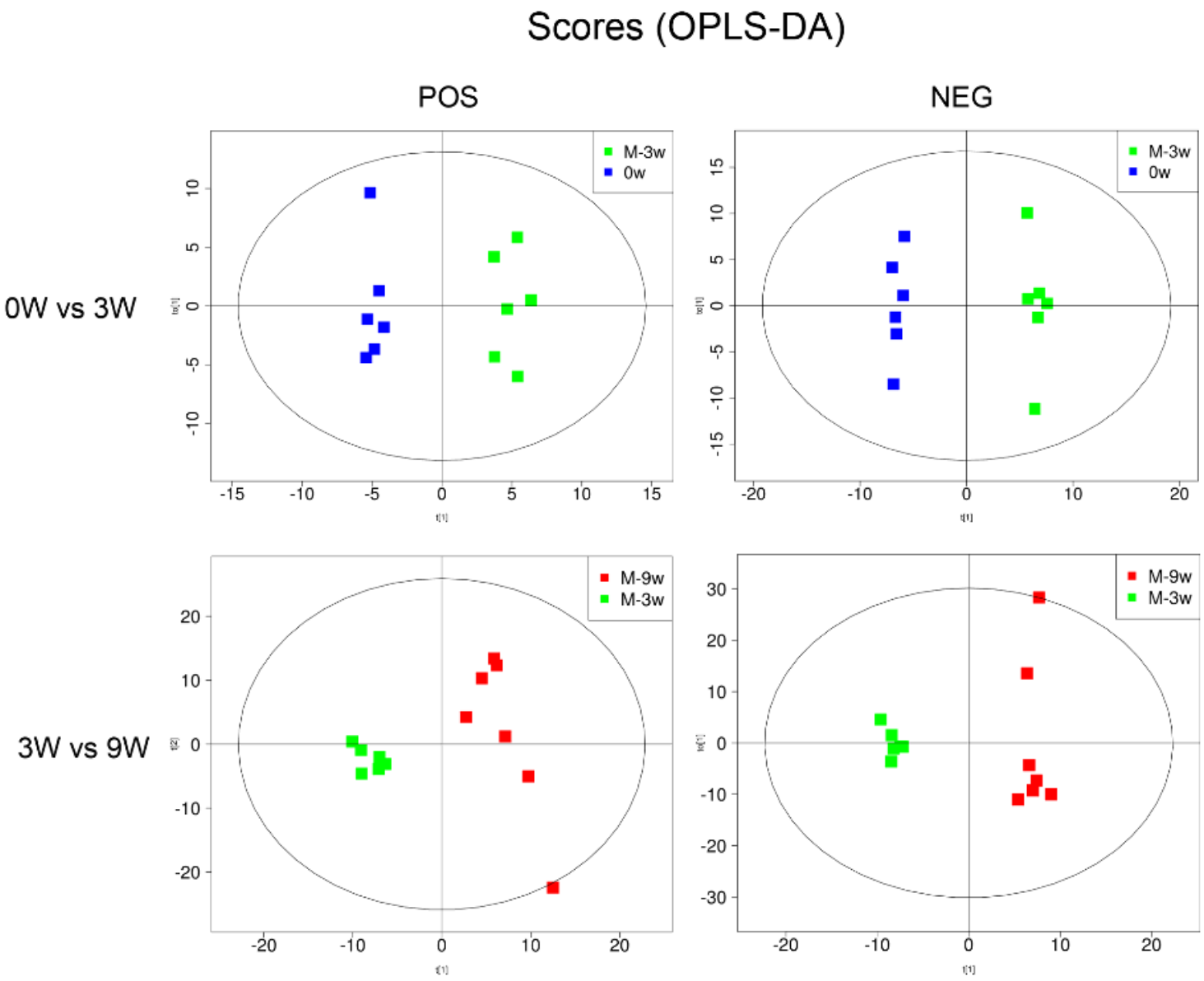

Figure 2

OPLS-DA analysis of metabolites by a solvent system under positive and negative ion modes. Spots in blue show samples from the 0 week group (0 W, n=6); spots in green indicate samples from the 3-week after TAC surgery group (3 W, n=6); spots in red indicate samples from the 9-week after TAC surgery group (9 W, n=7).

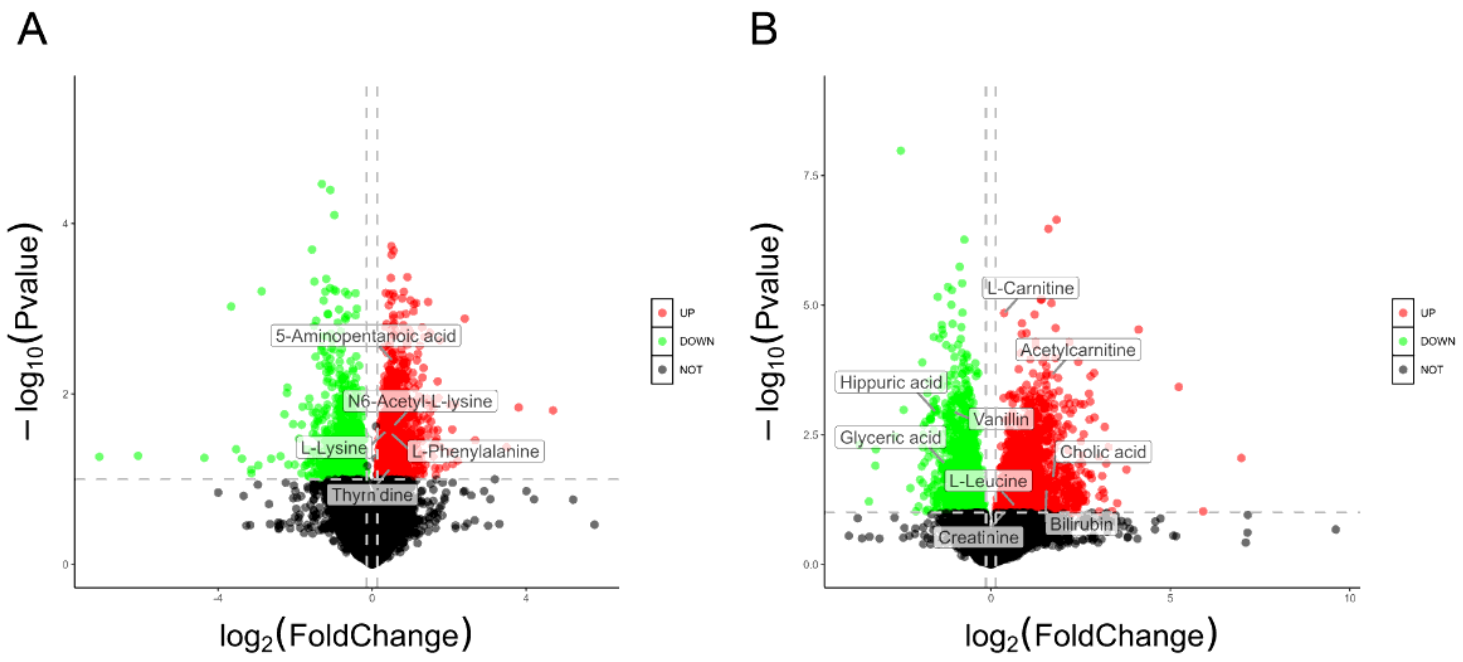

Figure 3

The clustering results of hierarchical cluster analysis based on the significantly different metabolites between groups under positive and negative models. A: cluster results of 0 week vs 3 week; B: cluster results of 3 week group vs 9 week group.

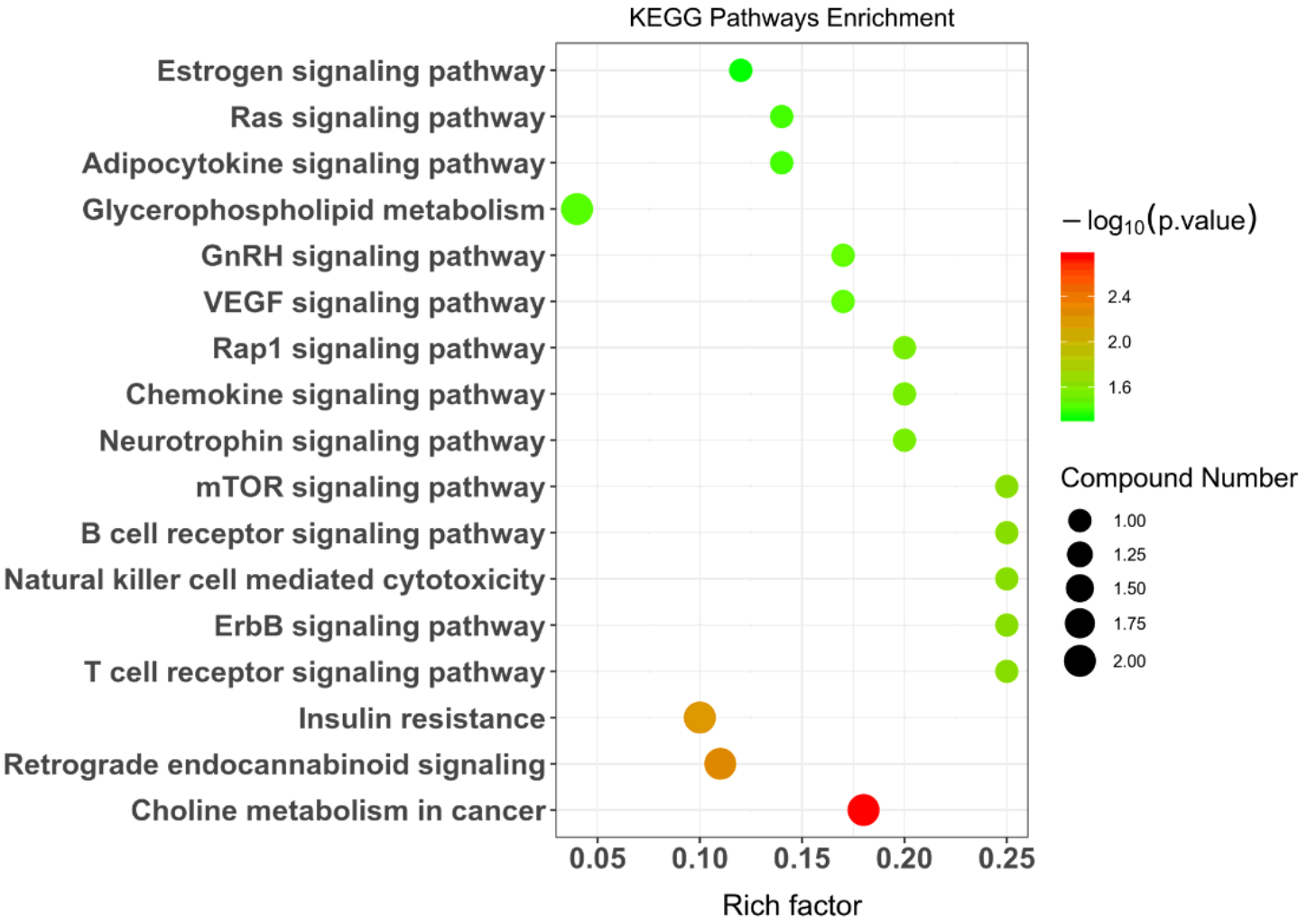

Figure 4

Enriched KEGG pathways between 3 W and 9 W presented by bubble diagram after TAC surgery based on significantly different metabolites.

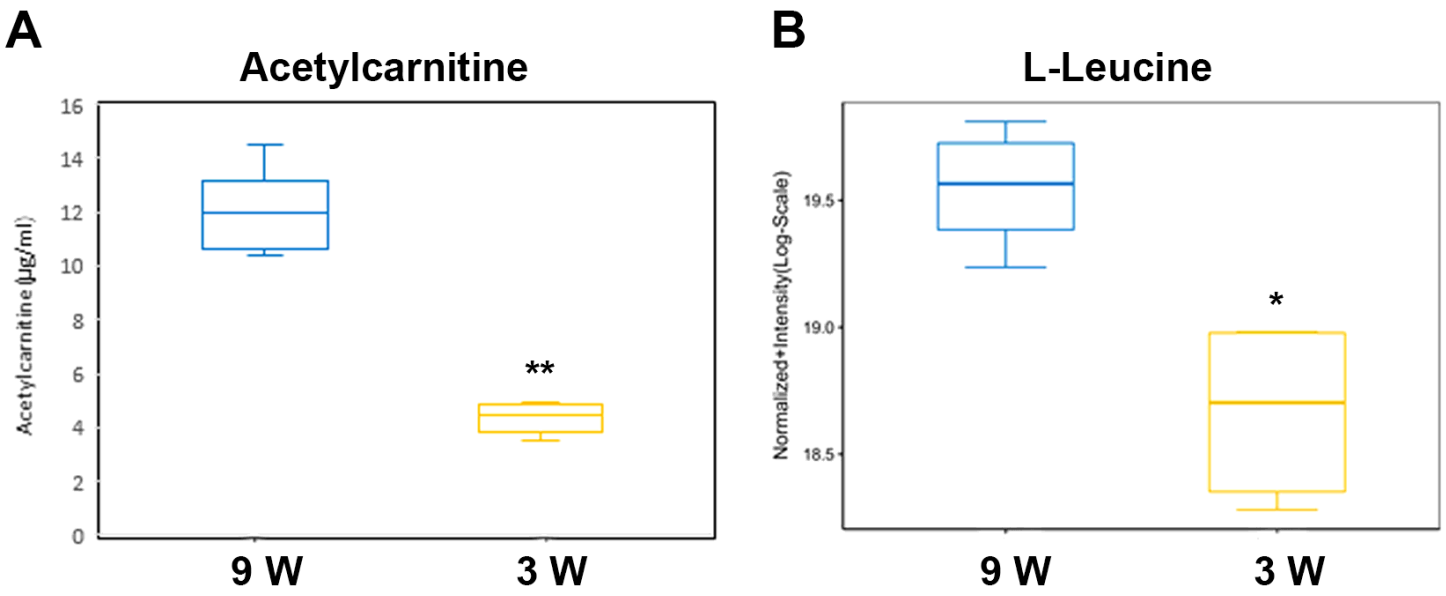

Figure 5

Plasma levels of acetylcarnitine and L-leucine. A: Plasma levels of acetylcarnitine confirmed by ELISA assay with the sensitivity of 7.1 pg/ml; The plasma levels of acetylcarnitines increased significantly at 9 W compared with 3 W group (12.04±1.42μg/ml vs 4.14±0.43 ug/ml, p□0.01); B: Plasma levels of L-leucine confirmed by target metabolic analysis. The normalized intensity of L-Leucine increased significantly at 9 W compared with 3W group. * p□0.05, ** p□0.01.